Evidence of PbI$_2$-Containing Debris Upon P2 Nanosecond Laser Patterning of Perovskite Solar Cells

Christof Schultz , Felix Schneider, Antje Neubauer, Andreas Bartelt, Marko Jošt, Bernd Rech, Rutger Schlatmann , Steve Albrecht, and Bert Stegemann

Abstract—Laser-based patterning for monolithic serial interconnection of metal halide perovskite (MHP) solar cells is a key process for industrial manufacturing of large-scale MHP solar panels. It requires reliable patterning process parameters to achieve low interconnection losses and, thus, high efficiencies. Here, P2 laser patterning of the perovskite layer was obtained by laser ablation using conventional nanosecond laser pulses at systematically varied laser fluences. The correlation of the laser impact to the morphology, composition, and electrical functionality was analyzed in detail by several surface-analytical techniques. The occurrence of laser-induced periodic surface structures and microdroplets at the bottom of the trenches indicates that material removal via stress-assisted ablation is strongly influenced by thermal processes. The formation of PbI$_2$-containing residuals was evidenced, possibly causing contact resistance losses through the P2 interconnect. These results contribute to the identification of loss factors in laser-based serial interconnection of perovskite solar cells and to further process optimization for upscaling to industrial module sizes.

Index Terms—Ablation, debris, laser, perovskite, P2, patterning, residuals.

I. INTRODUCTION

INORGANIC–ORGANIC metal halide perovskites (MHPs) are very promising candidates for absorbers in low-cost solar cells [1], [2]. The main reason is its outstanding physical properties such as strong optical absorption, high charge carrier mobility, and excellent diffusive transport properties [3]. Perovskites solar cells use an absorber layer of general ABX$_3$ stoichiometry with a wide compositional range of compounds, where A = methylammonium (MA), formamidinium (FA), cesium (Cs) and B = Pb^{2+}, Sn^{2+}, Ge^{2+}, Ni^{2+}; X = iodine (I), bromine (Br), chlorine (Cl) are most commonly used [4], allowing for a tunability of the bandgap by variation of the composition [4], [5]. Thus, MHP solar cells have not only been identified as promising candidates for single-junction solar cells, but also for stacked tandem devices with one or two perovskite absorber layers [1], [4], [6]. Due to extensive research, initial power conversion efficiencies (PCE) greater than 22% [7] and stabilized efficiencies above 20% were achieved at laboratory scale with solution-processed solar cells [8].

The upscaling from small laboratory scales to industry relevant sizes requires serial interconnection of solar cells to increase the output voltage and to limit the current. Over the last years, laser processing has become a key technology in thin-film photovoltaics to achieve monolithic serial interconnection, which involves alternating layer deposition and layer patterning (so-called patterning steps P1, P2, P3) [9]. Thereby, the solar cell layers are patterned by very fine lines by selective material removal alternating with layer deposition. The P1 and the P3 scribes are used to isolate the back and front contact, and thereby determine the width of the cells, while the absorber-opening scribe (P2) enables the interconnection between the back contact and front contact of the adjacent cells. The area between the outer edges of the P1 and P3 lines is electrically inactive (so-called dead area). The range of the dead area might extend up to 100 μm away from the scribe and, thus, be notably larger than visual inspection suggests [10]. However, in order to achieve a high aperture ratio, the dead area should be as small as possible. The beneficial utilization of lasers allows highly reproducible patterning, and thereby it is advantageous in comparison to conventional needle-based patterning in terms of tool wear, accuracy, and process quality [11].

For common thin-film technologies, such as thin-film Si and CIGSe, the interaction of the laser irradiation with the specific constituent layers has been extensively studied [10], [12], and laser patterning is well-established even in industrial production [13]. However, the fabrication of large-area perovskite solar modules requires additional engineering efforts to

customize these well-established process parameters and to properly interconnect adjacent cells. In general, successful P1 and P3 patterning is characterized by a sufficiently high isolation resistance across the corresponding scribe, whereas successful P2 patterning requires a clean and smooth bottom of the trench— in order to enable lowest contact resistances—without damages of the underlying front contact layer or modified edges of the surrounding absorber material.

A few groups have reported already on successful laser-based serial interconnection and perovskite minimodule fabrication. A first monolithically series interconnected minimodule based on the mesoporous perovskite cell concept was presented in 2014 by Matteocci *et al.* reaching a PCE of ∼5.1% at an aperture area of ∼10 cm^2 [14]. At this early state, the interconnection was enabled by means of lift-off, chemical etching the P2 and masking of the P3 step. In 2015, Razza *et al.* showed a 100 cm^2 mesoporous MHP minimodule with a PCE of 4.3% [15]. Thereby, P2 patterning was carried out by a combination of lift-off and laser processing, the cell area was defined by masking. In the same year, a first fully laser-patterned minimodule was presented by Moon *et al.* reaching a PCE of about 6.6% at 5 cm^2 mesoporous MHP absorber material [16]. Palma *et al.* even increased the aperture area of the mesoporous perovskite absorber layer up to 14.5 cm^2 achieving 9.3% efficiency and a rather high aperture ratio of 95%. Recently, IMEC and Solliance [17] published their latest results and achieved a PCE of 12.4% at a 16 cm^2 minimodule, presumable also with a mesoporous structured perovskite absorber. According to these very promising results, particularly the ablation of the absorber layer by means of the P2 scribe appears still challenging and is apparently the origin of a distinct performance drop due to resistive losses, when advancing from the cell to module. Moreover, the shown rather low open-circuit voltages (V_{oc}) and comparatively low fill factor (FF) underline the assumption of resistive losses between neighboring cells, most likely due to laser-related effects, including debris- and laser-induced damage of the underlying layer.

Apparently, the P2 patterning is challenging for all laser-based approaches apparently irrespective of the cell concept (meso-porous, planar) or the MHP absorber composition, though most work has been focused yet on the mesoporous concept. Thus, it is assumed that the thermal sensitivity of the inorganic–organic perovskite compound [18], [19] might impair successful P2 laser patterning. Palma *et al.* [20] recommend a rather broad P2 scribe line, similar to the approach of Moon *et al.* [16], whereas Turan *et al.* [21] prefer multipassing in order to overcome high series resistances and to enable low-contact resistances by P2 patterning.

Thus, the objective of this work is to deliberately control the thermal impact of nanosecond (ns) laser pulses for the preparation of the P2 interconnects by optimization of the incident laser fluence, with the focus on the planar perovskite cell concept. Moreover, we aim to elucidate the results of the laser–matter interaction and to understand their correlation to the morphological, chemical, electrical, and structural properties of the laser-patterned area. Particular emphasis is put on the characterization of the bottom of the trench, since even for scribe lines, which are visually free of debris, residuals created by the laser impact are assumed to remain impeding a low contact
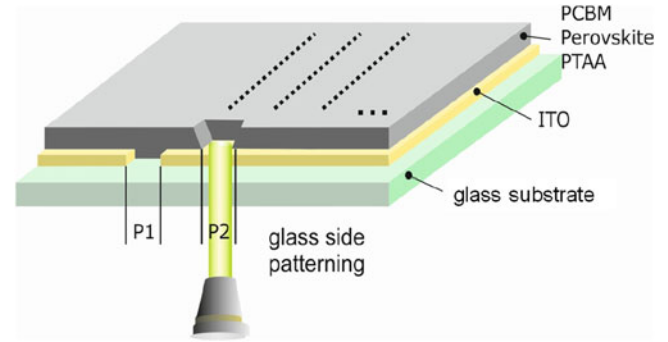

Fig. 1. Schematic illustration of the experimental approach. Multiple lines were patterned into the perovskite layer by using ns laser pulses at systematically varied energy densities.

resistance. Thus, the determination and localization of these residuals are considered to be essential to optimize the laser patterning processes. In accordance with the well-established patterning process for amorphous silicon, the P2 laser patterning for the perovskite-based cells was carried out from the glass side by means of a cost-effective nanosecond (ns) laser. The avoidance of plasma shielding [22] and the advantage of mechanically stress-assisted disintegration [23] enable selective ablation of the layer and make the glass side patterning regime putatively preferable.

Fig. 1 shows schematically the utilized sample layout, the P2 scribes were patterned line by line with systematically varied fluences.

For spatial analysis of the local conductivity, atomic force microscopy in the current-sensing mode (c-AFM) was chosen since it is a very efficient and versatile technique, which can be used to obtain locally resolved information about the morphology and the vertical conductivity between the AFM tip and to the substrate. The residuals were investigated by means of scanning electron microscope (SEM) images evaluating the morphology of the P2 bottom, whereas energy dispersive x-ray analysis (EDX) gives information about modifications of the local material composition. Moreover, the alteration of the composition of the absorber material within the trench is allocated to a new (stable) compound, and its relative composition as a function of the applied fluence is shown. Photoluminescence (PL) imaging was utilized for the locally resolved analysis of the optoelectronic properties, such as recombination processes and optical bandgaps, particularly at the bottom of the trenches and the surrounding material.

II. EXPERIMENTAL DETAILS

A. Sample Preparation

The perovskite solar cell deposition process was carried out by spin coating, resulting in a high reproducibility of the PCE on the 18% efficiency level, based on optimized deposition protocols from previous reports [24], [25]. For our experiments here, we fabricated two different sample designs in so-called "inverted" planar architecture (i.e., p–i–n geometry). First, methylammonium lead iodide (MAPbI$_3$) perovskite solar cells, using lead acetate and methylammonium iodide as precursors [25].

TABLE I
OVERVIEW OF THE APPLIED PROCESS PARAMETERS FOR PATTERNING

Parameter	
Wavelength (λ)	532 nm
Pulse duration (τ_p)	~ 30 ns
Diameter ($2\omega_0$)	28 µm ± 5 %
Pulse energy (E_p)	1.6 – 12.3 µJ
Fluence (F)	0.5 – 4.2 J/cm²
Overlap (OL)	~ 65%

The solar cell layer configuration was 1.1 mm glass, 140 nm ITO, 5 nm PTAA (hole selective contact), 270 nm perovskite, 50 nm PCBM, and 5 nm BCP (electron selective contact) [26]. Due to the continuous optimization of the perovskite preparation, we also investigated a "triple cation" perovskite sample consisting of a mixture of lead compounds (PbI$_2$/PbBr$_2$) and methylammonium bromide (MABr), formamidinium iodide (FAI), and cesium iodide (CsI) salts with a composition of Cs$_{0.05}$ (MA$_{0.17}$FA$_{0.83}$) $(100x)$ Pb (I$_{0.83}$Br$_{0.17}$)$_3$, which enables higher efficiency and stability against photochemical degradation [27]. The layer configuration of these samples is 1.1 mm glass, 120 nm ITO, 5 nm PTAA, ~700 nm perovskite, 23 nm C$_{60}$ plus 8 nm BCP, with C$_{60}$ and BCP thermally evaporated. For both sample designs, 100 nm Ag is deposited onto the stack via thermal evaporation as a counter electrode. The whole preparation was carried out under nitrogen atmosphere at atmospheric pressure to avoid absorber degradation [28].

B. Laser Patterning

For laser patterning of the solar cell layers, a patterning tool (Rofin Baasel Lasertech) equipped with a high-speed motion system was used. This system consists of high-precision linear motor drives for the *x*–*y* translation. The stages can be moved with velocities of up to 1.2 m/s. The patterning was carried out with an ns laser source emitting pulses with durations of about $\tau_p \approx 30$ ns at a wavelength of 532 nm. This wavelength is preferable for glass side patterning, due to the high transparency of the glass and the high absorption of this wavelength within the perovskite layer supporting the mechanically stress-assisted ablation [22]. Maximum pulse energy of 45 µJ is achieved at a repetition rate of 20 kHz, which can be varied up to 400 kHz, the spatial intensity distribution is Gaussian. The patterning was done line-by-line with systematically varied laser pulse energies, covering the range of incomplete ablation of the absorber layer up to the onset of front contact damaging. The applied laser fluence ranges from 0.5 to 4.2 J/cm² related to a laser beam diameter of $2\omega_0 \approx (28 \pm 5)$ µm. The pulse-to-pulse overlap (OL) was around 65% with respect to $2\omega_0$ at a pulse repetition rate of 20 kHz and was kept constant for all patterned lines. This pulse-to-pulse OL was chosen on the one hand to create a large interconnection area with minimal waists between adjacent laser shots and on the other hand to avoid excessive thermal input at the surrounding material and underlying ITO. An overview of the applied patterning parameters is given in Table I.

C. Characterization Techniques

The morphology and local conductivity of the P2 scribe were measured by a conductive atomic force microscope (c-AFM, NT-MDT NTEGRA) in the current sensing mode using a highly nitrogen-doped diamond tip. The surface was scanned at areas up to 50 µm × 50 µm under a bias voltage of 2 V, and the topography as well as the current signal was recorded simultaneously. For visual inspections of the laser patterns and modifications of the sample surface, a laser confocal microscope (OM, Keyence, VK-X250K) and an SEM (Hitachi S4100) were used. The latter one also enables the local detection of the elemental composition of the sample by means of EDX spectroscopy; the acceleration voltage was set to 5 kV. For detection of the spectrally resolved PL, a commercially available laser scanning microscope (Becker & Hickl, Simple-Tau) was used. The samples were excited by a ps laser at a wavelength of 2.63 eV (473 nm), which is well above the bandgap energy of the perovskite ~1.6 eV (~775 nm). Spectrally selective detection of the PL signal of the samples was done by specific filters.

III. RESULTS AND DISCUSSION

To open the absorber layer for monolithic interconnection, the P2 laser patterning was carried out through the glass substrate, as schematically shown in Fig. 1, with ns pulses at 532 nm. Thus, one can make use of the high difference between the absorptions coefficients of the front contact layer and the perovskite layer at 532 nm, which facilitates mechanical stress assisted ablation. For the P2 scribe, it is important to create a sufficiently large contact area for the interconnection of adjacent cells to enable low contact resistances. Therefore, a relatively high pulse-to-pulse OL is necessary. Furthermore, the bottom of the trench must be free of residuals, which might impede low contact resistances down to the front contact layer. To identify the optimal process window, the applied laser power was systematically varied, covering the range from incomplete ablation of the absorber layer (0.5 J/cm²) to the onset of ablation of the underlying ITO front contact layer (4.2 J/cm²). Thus, multiple lines were patterned in the perovskite layer, which was subsequently characterized by c-AFM, which is a powerful technique for probing local conductivity variations in heterogeneous samples with high spatial resolution [29]. Information on the local electronic properties is obtained by applying a bias voltage between the tip and the sample and sensing the resulting current. To identify optimal scribing conditions, the morphology of the sample surface as well as the spatially resolved, vertical conductivity was analyzed. A high current corresponds to a high conductivity.

The values of the average conductivity within the trenches for all applied laser fluences are summarized in the graph in Fig. 2. The results show that the conductivity increases within increasing fluence (up to a fluence of ~1.5 J/cm²) due to the ablation of the perovskite and the exposure of the ITO. Beyond 1.5 J/cm², the perovskite layer is completely ablated and an alteration of the ITO sets in, resulting in a decrease of the local conductivity.

Fig. 3(a) shows the morphology of the P2 scribe and its vicinity patterned with a laser fluence of 1.53 J/cm². The image shows a homogeneous trench with a nearly constant width of about
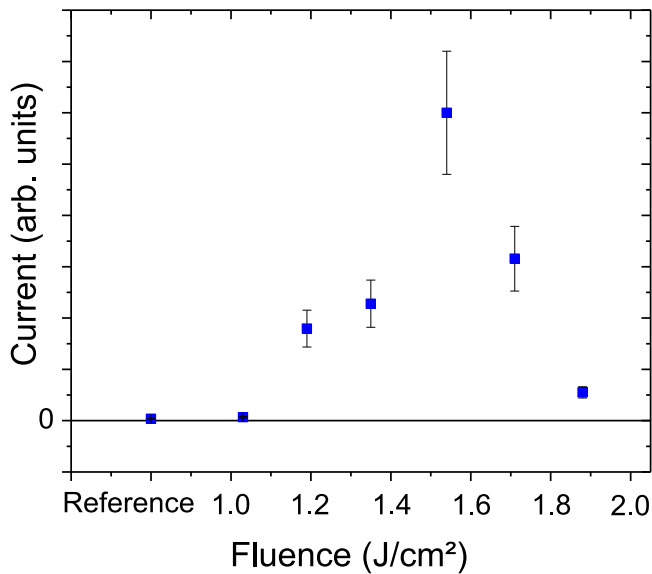
Fig. 2. Current between sample surface and c-AFM tip as a function of the applied laser fluence. The data points correspond to the average value within the laser-treated area.
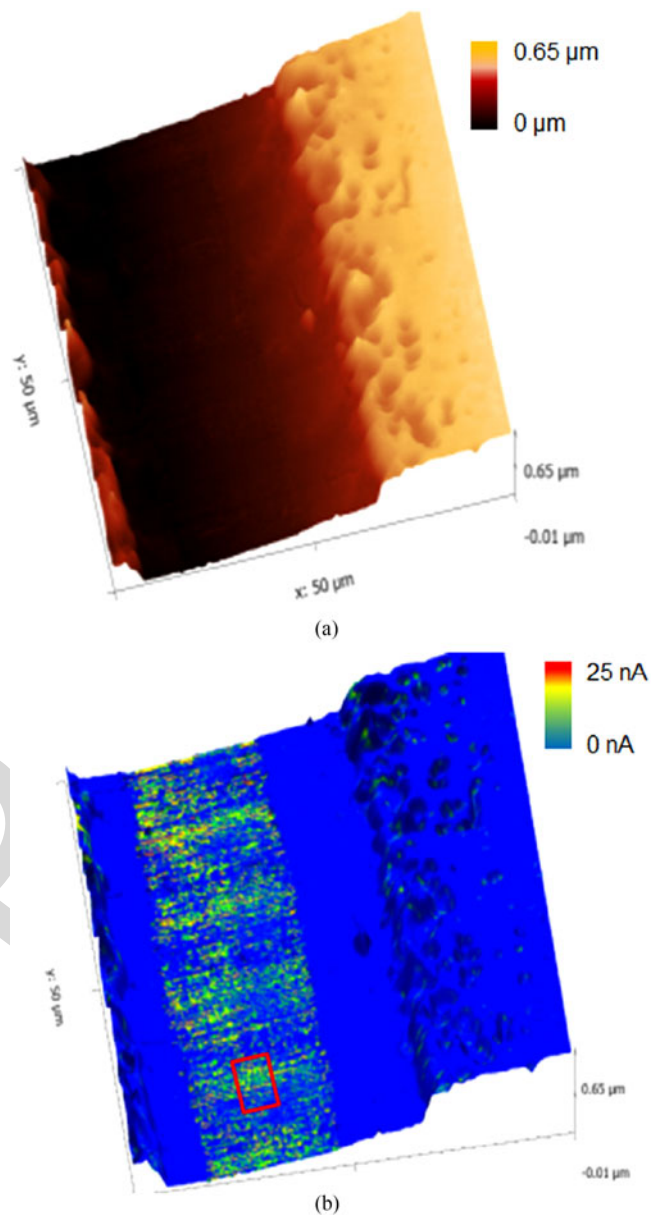

(a)

(b)

Fig. 3. (a) AFM topography. (b) Corresponding conductivity three-dimensional plots of a P2 laser-patterned trench, patterned at a fluence of $1.53\,J/cm^2$.

35 μm. The bottom appears clean and smooth as it is preferable for low-ohmic contact resistances. The slight modifications at the edges of the trench may result from the lateral heat flux during the patterning process and give a hint that lateral thermal effects might superimpose the mechanically stress-assisted ablation as it is known from glass side patterning of, e.g., amorphous silicon thin films [23]. Following this observation, the absorption of the laser energy not only results in mechanical stress and subsequent ablation but also in heating of the perovskite layer leading to decomposition and melting of the perovskite film.

The corresponding current image is obtained by applying a bias voltage between the tip and the ITO contact and sensing the resulting current. As shown in Fig. 3(b), it visualizes a clear difference in the local conductivity between the center of the bottom trench and the untreated area, due to the removal of the perovskite and the exposure of the ITO layer. Moreover, at the bottom of the trench, alternating regions with higher and lower conductivity are found, indicating the formation of a surface texture, which is not visible in the topography image [see Fig. 3(a)]. The cross-sectional SEM image in Fig. 4 shows the edge and the center of a trench patterned at an even higher fluence of $4.2\,J/cm^2$.

Here, the surface texture is clearly visible and can be identified as laser-induced periodic surface structures (LIPSS) [30], which are known to be formed by laser irradiation over a wide range of materials and laser process parameters particularly at high pulse-to-pulse OL [22], as was used for P2 patterning. Such structures are understood to originate from the interference of the incident laser light with the reflected or scattered light [31]. The LIPSS periodicity is approximately 580 nm and, thus, in the same order of the incident laser wavelength. Since these periodic structures also appear both in the SEM and the c-AFM image [cf., Fig. 3(b)], it is concluded that there is an incomplete material removal of the perovskite layer and an

elemental redistribution leading to the periodic formation of phases with different conductivities, what can be understood by the low melting points of lead and iodine (600 and 386 K) [32] and the low sublimation temperature of the organic compound [33]. We estimated for the ns laser pulses, even for fluences below $1.5\,J/cm^2$, that local temperatures might reach several hundreds of Kelvin above room temperature, which affects mainly the organic part of the perovskite compound and leads to a transformation into PbI_2.

This interpretation is further supported by the identification of droplets on the top of the front contact layer, as revealed in the SEM image in Fig. 4 for the sample patterned at high laser fluence. From these findings, it is concluded that for ns-laser-based P2 patterning, the material removal via stress-assisted ablation is strongly influenced by thermal processes.
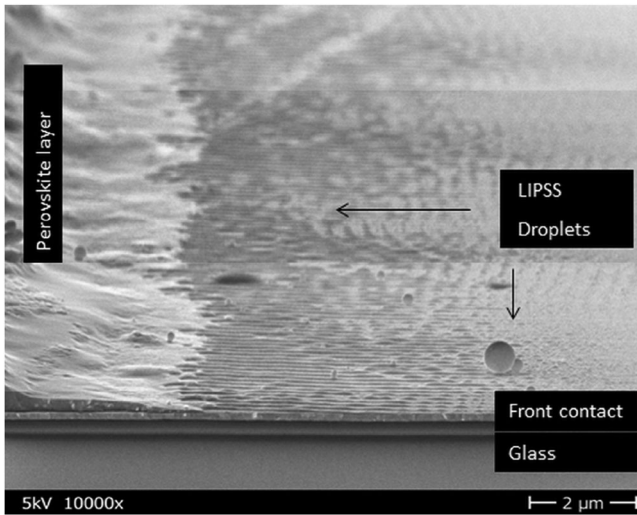
Fig. 4. SEM cross-section image of the edge and bottom of the laser scribed line, patterned at $4.2\,J/cm^2$. Image width: $12\,\mu m$, tilt: $10°$, and acceleration voltage: 5 kV.
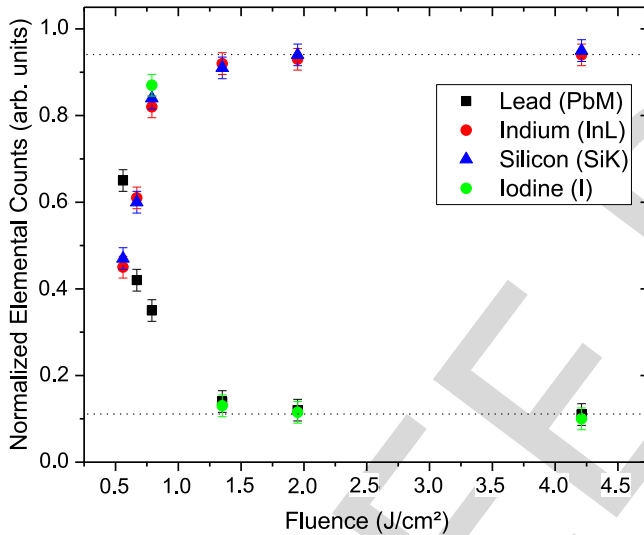

Fig. 5. Elemental composition within the P2 laser scribes as a function of the applied laser fluence. Shown are the elements I, In, Pb, and Si.

Fig. 6. Photoluminescence images of a P2 trench, patterned at $1.9\,J/cm^2$, revealing the emission originating. (a) Perovskite. (b) PbI₂. Spectral selectivity was achieved by specific filters. (a) 665 nm long pass. (b) 510/40 nm bandpass. Characteristic profiles across the P2 laser trenches correspond to the white lines and are given below the images.

To determine the elemental composition of the residuals at the bottom of the trench, all scribed lines were investigated by EDX.

Fig. 5 shows the corresponding elemental composition of the scribed lines as a function of the applied laser fluence as obtained from the relative peak intensities of the relevant elements.

As elemental references for the material composition within the scribed lines, the elements Pb, I, In, and Si were selected. Therefore, Pb and I represent the absorber materials, In the front contact, and Si the glass substrate. The results in Fig. 5 show that with increasing laser fluence the MHP layer is ablated. While the Pb and I concentration decreases with higher fluence, the In and the Si concentrations increase in the same way. However, even at high fluence, a Pb signal (about 10% of the total amount) is detected, indicating Pb-containing residuals at the bottom of the scribe.

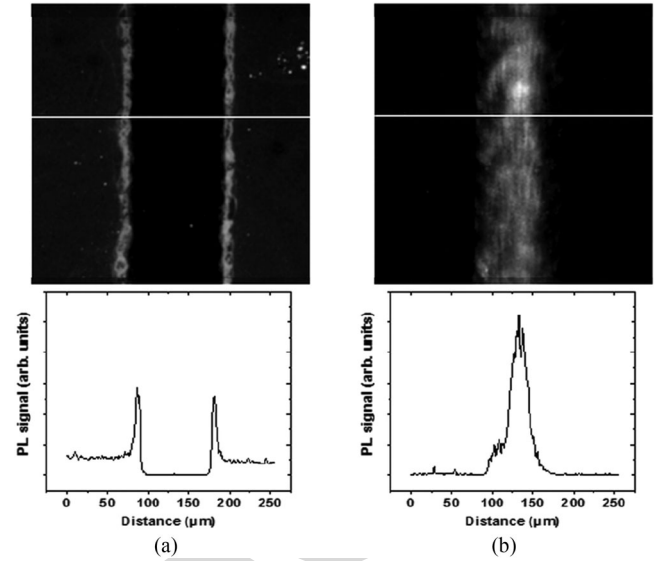With respect to the periodic structures shown in Figs. 3 and 4, it will be now clarified if the higher conductivity is due to remaining well-conducting lead-rich phases or to regions where the front contact is exposed and the remaining residuals impede a high conductivity (low contact resistance). To address this issue, spectrally resolved PL imaging was performed. The corresponding images of a sample prepared at a fluence ($1.9\,J/cm^2$) close to the one resulting in the conductivity maximum ($1.5\,J/cm^2$) are shown in Fig. 6.

The PL distribution of a P2 scribing line and its vicinity after filtering with a long-pass filter that transmits wavelengths above 665 nm is shown in Fig. 6(a). Thus, the emission of the main transition of the perovskite layer at 780 nm (1.59 eV) is detected. The line scan below corresponds to the white line in the PL image and shows that at the bottom of the trench the PL signal of the perovskite vanishes, indicating the absence of perovskite. A further distinct feature is the raised PL intensity at the edges of the scribed line, which can be attributed to the removed electron extraction layer (C_{60}/PCBM) close to the scribe allowing for an increased perovskite PL intensity [24]. Further analysis of the edges by means of confocal optical microscopy shows only very little ridges; thus, focus-related effects regarding the signal detection can be excluded. However, further investigations to quantify this effect are in progress.

In contrast, the PL image in Fig. 6(b) was acquired using a bandpass filter with a nominal center wavelength of 510 nm and a bandwidth of 40 nm. This filter enables the detection of the PL signal of PbI₂ (main transition at 529 nm at 300 K [34]) while blocking the PL signal of the perovskite. As is seen, a distinct PL signal is found within the scribed line, apparently originating from PbI₂-based residuals, which are formed upon laser impact and remain in the trench after P2 laser patterning. This interpretation is in agreement with x-ray diffraction

measurements by Bayer *et al.*, who observed structural decomposition of MHP due to ns laser patterning, resulting in the formation of PbI_2 [35]. PbI_2 formation in lead-containing perovskite layers has been focused a lot of attention and its role for the performance of the device has been controversially discussed. It was proposed that a degradation of the lead-containing perovskite to PbI_2 might occur in air or vacuum, with excessive heat or humidity facilitating this process [36]. Some beneficial effects are ascribed to the presence of PbI_2, such as passivation of perovskite grain boundaries [37], [38], increasing the shunt resistance of the active layer and reducing the ion mobility [39]. However, detrimental effects on the photostability were also found to be caused by excess PbI_2 [40]. Moreover, ns P2 laser ablation was observed to be followed by redeposition of ablated material.

Taking all this observation into account, we conclude that thermal effects lead to the decomposition of the organic/inorganic hybrid material resulting in a formation of PbI_2 with a periodically structured morphology and possibly the redeposition of PbI_2 debris. Thus, it must be assumed that the remaining PbI_2 within the trench might act as a barrier for the charge carrier transport [37] due to its rather high resistivity of 108–1010 $\Omega \cdot$cm [41], [42] and its comparatively large band gap of 2.34 eV [34], thus impeding low-contact resistances. These findings can be generalized to all investigated absorber layer compositions in the "inverted" planar architecture. Process windows and results from SEM and EDX measurements are consistent. Even the slightly thicker absorber layer used for the triple cation sample has a negligible influence on the absorption behavior.

IV. Summary and Conclusion

P2 laser patterning through the glass substrate by ns laser pulses for monolithic series interconnection of MHP solar cells was investigated over a wide range of laser fluences. Successful selective laser ablation from the glass side is demonstrated, though at the bottom of the scribed lines periodically structured, residual composed of PbI_2 remains even at higher fluences. These features form periodic surface structures (LIPSS), which exhibit regions of higher and lower conductivity, and thus impede low contact resistances for the P2 interconnect. It is concluded that the comparatively poor conductivity of PbI_2 hinders lower contact resistances as they are essential for successful monolithic series interconnection.

The occurrence of LIPSS and in addition microdroplets at the uncovered front contact layer indicate that material removal for P2 patterning via stress-assisted ablation is strongly influenced by thermal processes. Thus, further extensive work is required to overcome these drawbacks and to adjust the process windows for industrial manufacturing. Currently, further process optimization is in progress evaluating shorter laser pulse durations to avoid thermal effects (i.e., heat accumulation) and different wavelengths for material excitation above and below the optical bandgap to further improve P2 patterning and to achieve lowest contact resistances.

References

[1] S. Albrecht *et al.*, "Monolithic perovskite/silicon-heterojunction tandem solar cells processed at low temperature," *Energy Environ. Sci.*, vol. 9, pp. 81–88, 2016.

[2] E. L. Unger, "The PV-researcher's siren: Hybrid metal halide perovskites," *Curr. Opinion Green Sustain. Chem.*, vol. 4, pp. 72–76, 2017.

[3] J. S. Manser, J. A. Christians, and P. V. Kamat, "Intriguing optoelectronic properties of metal halide perovskites," *Chem. Rev.*, vol. 116, pp. 12956–13008, 2016.

[4] E. L. Unger *et al.*, "Roadmap and roadblocks for the band gap tunability of metal halide perovskites," *J. Mater. Chem. A*, vol. 5, pp. 11401–11409, 2017.

[5] Q. A. Akkerman *et al.*, "Tuning the optical properties of cesium lead halide perovskite nanocrystals by anion exchange reactions," *J. Amer. Chem. Soc.*, vol. 137, pp. 10276–10281, 2015.

[6] T. Todorov *et al.*, "Monolithic perovskite-CIGS tandem solar cells via in situ band gap engineering," *Adv. Energy Mater.*, vol. 5, 2015, Art. no. 1500799.

[7] N.-G. Park, "Methodologies for high efficiency perovskite solar cells," *Nano Convergence*, vol. 3, pp. 1–13, 2016.

[8] Ecole Polytechnique Fédérale de Lausanne, "Perovskite solar cells reach record long-term stability, efficiency over 20%," Science Daily, 2017.

[9] A. Compaan, I. Matulionis, and S. Nakade, "Optimization of laser scribing for thin-film PV modules," Univ. Toledo, Toledo, OH, USA, Final Tech. Prog. Rep., 1998, p. 43.

[10] C. Schultz *et al.*, "Revealing and identifying laser-induced damages in CIGSe solar cells by photoluminescence spectroscopy," *IEEE J. Photovolt.*, vol. 7, no. 5, pp. 1442–1449, Sep. 2017.

[11] L. Rakocevic *et al.*, "Interconnection optimization for highly efficient perovskite modules," *IEEE J. Photovolt.*, vol. 7, no. 1, pp. 404–408, Jan. 2017.

[12] C. Schultz *et al.*, "Laser-induced local phase transformation of CIGSe for monolithic serial interconnection: Analysis of the material properties," *Sol. Energy Mater. Sol. Cells*, vol. 157, pp. 636–643, 2016.

[13] G. Heise, A. Heiss, H. Vogt, and H. P. Huber, "Ultrafast lasers improve the efficiency of CIS thin film solar cells," *Phys. Procedia*, vol. 39, pp. 702–708, 2012.

[14] F. Matteocci *et al.*, "Solid-state solar modules based on mesoscopic organometal halide perovskite: A route towards the up-scaling process," *Phys. Chem. Chem. Phys.*, vol. 16, pp. 3918–3923, 2014.

[15] S. Razza *et al.*, "Perovskite solar cells and large area modules (100 cm²) based on an air flow-assisted PbI_2 blade coating deposition process," *J. Power Sources*, vol. 277, pp. 286–291, 2015.

[16] S.-J. Moon *et al.*, "Laser-scribing patterning for the production of organometallic halide perovskite solar modules," *IEEE J. Photovolt.*, vol. 5, no. 4, pp. 1087–1092, Jul. 2015.

[17] IMEC and Solliance, "IMEC and Solliance's perovskites PV modules achieve 12.4%," 2017. [Online]. Available: https://solliance.eu/perovskite-modules-achieve-12-4pct/

[18] E. J. Juarez-Perez, Z. Hawash, S. R. Raga, L. K. Ono, and Y. B. Qi, "Thermal degradation of $CH_3NH_3PbI_3$ perovskite into NH_3 and CH_3I gases observed by coupled thermogravimetry-mass spectrometry analysis," *Energy Environ. Sci.*, vol. 9, pp. 3406–3410, 2016.

[19] A. E. Williams *et al.*, "Perovskite processing for photovoltaics: A spectro-thermal evaluation," *J. Mater. Chem. A*, vol. 2, pp. 19338–19346, 2014.

[20] A. L. Palma *et al.*, "Laser-patterning engineering for perovskite solar modules with 95% aperture ratio," *IEEE J. Photovolt.*, vol. 7, no. 6, pp. 1674–1680, Nov. 2017.

[21] B. Turan, A. Huuskonen, I. Kühn, T. Kirchartz, and S. Haas, "Cost-effective absorber patterning of perovskite solar cells by nanosecond laser processing," *Solar RRL*, vol. 1, 2017, Art. no. 1700003.

[22] D. W. Bäuerle, *Laser Processing and Chemistry*. New York, NY, USA: Springer, 2013, p. 281.

[23] J. Bovatsek, A. Tamhankar, R. Patel, N. Bulgakova, and J. Bonse, "Thin film removal mechanisms in ns-laser processing of photovoltaic materials," *Thin Solid Films*, vol. 518, pp. 2897–2904, 2010.

[24] L. Kegelmann *et al.*, "It takes two to tango – Double-layer selective contacts in perovskite solar cells for improved device performance and reduced hysteresis," *ACS Appl. Mater. Interfaces*, vol. 9, pp. 17245–17255, 2017.

[25] M. Jošt *et al.*, "Efficient light management by textured nanoimprinted layers for perovskite solar cells," *ACS Photon.*, vol. 4, pp. 1232–1239, 2017.

[26] M. Stolterfoht *et al.*, "Approaching the fill factor Shockley-Queisser limit in stable, dopant-free triple cation perovskite solar cells," *Energy Environ. Sci.*, vol. 10, pp. 1530–1539, 2017.

[27] M. Saliba *et al.*, "Cesium-containing triple cation perovskite solar cells: Improved stability, reproducibility and high efficiency," *Energy Environ. Sci. Adv.*, vol. 9, pp. 1989–1997, 2016.

[28] Z. Song *et al.*, "Perovskite solar cell stability in humid air: Partially reversible phase transitions in the PbI$_2$-CH$_3$NH$_3$I-H$_2$O system," *Adv. Energy Mater.*, vol. 6, 2016, Art. no. 1600846.

[29] B. Stegemann, J. Čermák, B. Rezek, J. Kočka, and M. Schmidt, "Silicon nanodot layers for photovoltaic application: Size/Density control and electrical properties," *Zeitschrift Phys. Chem.*, vol. 228, pp. 543–556, 2014.

[30] J. Bonse, S. Höhm, S. Kirner, A. Rosenfeld, and J. Krüger, "Laser-induced periodic surface structures (LIPSS) - A scientific evergreen," *IEEE J. Sel. Top. Quantum Electron.*, vol. 23, no. 3, May/Jun. 2017, Art. no. 9000615.

[31] K. Sugioka and Y. Cheng, "Ultrafast lasers - Reliable tools for advanced materials processing," *Light Sci. Appl.*, vol. 3, 2014, Art. no. e149.

[32] W. M. Haynes, *CRC Handbook of Chemistry and Physics*. Boca Raton, FL, USA: CRC Press, 2014.

[33] A. Dualeh, P. Gao, S. I. Seok, M. K. Nazeeruddin, and M. Grätzel, "Thermal behavior of methylammonium lead-trihalide perovskite photovoltaic light harvesters," *Chem. Mater.*, vol. 26, pp. 6160–6164, 2014.

[34] R. Ahuja *et al.*, "Electronic and optical properties of lead iodide," *J. Appl. Phys.*, vol. 92, pp. 7219–7224, 2002.

[35] L. Bayer *et al.*, "Morphology and topography of perovskite solar cell films ablated and scribed with short and ultrashort laser pulses," *Appl. Surf. Sci.*, vol. 416, pp. 112–117, 2017.

[36] Q. Sun *et al.*, "Role of microstructure in oxygen induced photodegradation of methylammonium lead triiodide perovskite films," *Adv. Energy Mater.*, vol. 7, 2017, Art. no. 1700977.

[37] T. J. Jacobsson *et al.*, "Unreacted PbI$_2$ as a double-edged sword for enhancing the performance of perovskite solar cells," *J. Amer. Chem. Soc.*, vol. 138, pp. 10331–10343, 2016.

[38] L. Wang, C. McCleese, A. Kovalsky, Y. Zhao, and C. Burda, "Femtosecond time-resolved transient absorption spectroscopy of CH$_3$NH$_3$PbI$_3$ perovskite films: Evidence for passivation effect of PbI$_2$," *J. Amer. Chem. Soc.*, vol. 136, pp. 12205–12208, 2014.

[39] T. Du *et al.*, "Formation, location and beneficial role of PbI$_2$ in lead halide perovskite solar cells," *Sustain. Energy Fuels*, vol. 1, pp. 119–126, 2017.

[40] F. Liu *et al.*, "Is excess PbI$_2$ beneficial for perovskite solar cell performance?" *Adv. Energy Mater.*, vol. 6, 2016, Art. no. 1502206.

[41] H. Henisch and C. Srinivasagopalan, "Properties of semiconducting lead iodide," *Solid State Commun.*, vol. 4, pp. 415–418, 1966.

[42] C. De Blasi *et al.*, "Trapping levels in PbI$_2$," *Solid State Commun.*, vol. 25, pp. 149–153, 1978.

Felix Schneider received the bachelor's degree in renewable energies from the University of Applied Sciences (HTW) Berlin, Germany, in 2015, and the master's degree in renewable energies in 2017 from the HTW Laser Research Group, Competence Center Thin-Film- and Nanotechnology for Photovoltaics Berlin, Berlin, Germany, where he focused on the serial interconnection of perovskite solar cells via laser patterning.

During his thesis, he worked with the PI Photovoltaik Institut Berlin, Berlin, Germany, on solar module testing and evaluation. Since 2018, he has been working with the TÜV Rheinland Industrie Service, Berlin, Germany.

Antje Neubauer studied chemistry at Humboldt University, Berlin, Germany. She received the Ph.D. degree in physics from Technical University, Cottbus, Germany, in 2010.

She worked in ultrafast spectroscopy of dye-sensitized solar cells with Helmholtz Centre Berlin, Berlin, Germany. Subsequent postdoctoral positions at Helmholtz Centre Berlin and University of Rostock focused on time-resolved spectroscopy of solar energy materials. Since 2015, she has been an Application Scientist for time-correlated single photon counting with Becker & Hickl GmbH, Berlin, Germany.

Andreas Bartelt received the Ph.D. degree from the Free University of Berlin, Berlin, Germany, where he focused on laser-driven chemistry induced by tailored femtosecond laser pulses.

He works in the field of laser chemistry and material sciences. Time-resolved spectroscopy using lasers and synchrotron x-rays was at the core of his Postdoctoral research at Princeton University, Lawrence Berkeley National Laboratories, and Helmholtz Center Berlin, investigating novel thin-film photovoltaic materials. He has been a Full Professor with the University of Applied Sciences, Berlin, Germany, since 2016. His main research interests include femtosecond spectroscopy and material processing of organic–inorganic hybrid and perovskite solar cells.

Christof Schultz received the diploma and master's degrees in renewable energies from the University of Applied Sciences, Berlin, Germany, in 2008 and 2014, respectively.

In 2010, he joined the HTW Laser Research Group, Competence Center Thin-Film- and Nanotechnology for Photovoltaics Berlin, Berlin, Germany, as a Specialist for laser applications. His current research interests include laser processing, laser spectroscopy, and characterization of CIGSe solar cells; for his Ph.D. studies, he focused on laser patterning of inorganic–organic perovskite solar cells as well as laser-induced damages in order to optimize the laser patterning.

Marko Jošt received the Ph.D. degree from the University of Ljubljana, Ljubljana, Slovenia, and Technical University Berlin, Berlin, Germany, where he investigated light management in solar cells.

He is currently a Postdoctoral Researcher with the Young Investigator Group Perovskite Tandem Solar Cells, Helmholtz-Zentrum Berlin, Berlin, Germany. His current research interest focuses on improving the efficiency of monolithic perovskite/silicon tandem solar cells, with an emphasis on optical optimization and interface engineering.

Bernd Rech studied physics at Heidelberg University, Heidelberg, Germany, and RWTH Aachen, Aachen, Germany. He received the Ph.D. degree in physics in 1997.

From 1999 to 2006, he was the Leader of a group specialized in solar cell technology with the Institute of Photovoltaics, Forschungszentrum Jülich. He was appointed as a Professor with the Faculty of Electrical Engineering and Computer Science, Technische Universität Berlin, in 2007. Since 2008, he has been the Spokesperson of the research program renewable energies of the Helmholtz Association. From 2006 to 2017, he was the Head of the Institute of Silicon Photovoltaics, Helmholtz-Zentrum Berlin (HZB), Berlin, Germany, and the Spokesperson of the division renewable energies from 2011 to 2017. He and his team focused on the development of highly efficient and affordable thin-film silicon solar cells and new material combinations for producing tandem solar cells. Since May 2017, he has been the Acting Scientific Director of the HZB.

Dr. Rech was elected member of Acatech (National Academy of Science and Engineering) in 2017.

Rutger Schlatmann received the Ph.D. degree in physics, working on X-ray multilayer mirrors, from the FOM Institute Amolf, Amsterdam, The Netherlands, in 1995.

From 1996 to 1999, he worked on high strength polymer fibers as a Research Scientist for Akzo Nobel. From 1999 to 2008, he was the R&D Manager with Helianthos BV, a company developing flexible thin-film Si solar modules. Since 2008, he has been the Director of the Center for Technology Transfer in Thin-Film- and Nanotechnology for Photovoltaics, Helmholtz-Zentrum Berlin, Berlin, Germany. Since 2012, he has held a Full Professorship (W3) with the University of Applied Sciences Berlin, Berlin, Germany. His research interests focus on all aspects of Si heterojunction and CIGS-based solar cells, including multijunction cells, new concepts for light capture and conversion (e.g., solar fuels, solar-driven hydrogen generation), alternatives to standard absorber layer formation, and on and offline analytics. His main focus is on research topics that are ready to move from proof of principle to proof of concept.

Dr. Schlatmann is a Member of the European Technology and Innovation Platform PV Steering Committee as well as the Vice President of the Berlin Brandenburg Energy Network, and a Member of various national and international conference and scientific evaluation committees.

Steve Albrecht received the Ph.D. degree in physics from the University of Potsdam, Potsdam, Germany.

He has been leading a young investigator group for perovskite-based multijunction photovoltaics at Helmholtz Center Berlin, Berlin, Germany, since 2016. In 2014, he joined Helmholtz Center Berlin, as a Postdoc until his young investigator group was founded. In 2017, he managed the build-up of the HySPRINT Innovation Lab for perovskite solar cells at Helmholtz Center Berlin, which is under operation now. Recently, his group developed a two-terminal, monolithic perovskite/silicon tandem solar cell with a certified efficiency of 25%.

Dr. Albrecht was a recipient of the Carl-Ramsauer-Prize and the Young Researcher Prize of the Berlin Physical Society and the Leibniz-Kolleg Potsdam, respectively, for his Ph.D. work on organic solar cells.

Bert Stegemann studied physics and optical sciences at the Humboldt University Berlin, Berlin, Germany, and the University of Arizona, Tuscon, AZ, USA. He received the Ph.D. degree in physical chemistry.

After completing his Ph.D. degree, he worked on several research projects in the fields of laser applications, material sciences, and photovoltaics. Since 2009, he has held a Full Professorship for photovoltaics with the University of Applied Sciences Berlin (HTW), Berlin, Germany, and is the Head of the HTW Laser Technology Lab, Competence Center Thin-Film- and Nanotechnology for Photovoltaics Berlin. His current research interests include laser processing, laser spectroscopy, and characterization of CIGSe, perovskite, and Si heterojunction solar cells as well as wet-chemical processing and interface passivation.

QUERIES 700

Q1. Author: Please confirm or add details for any funding or financial support for the research of this article. 701
Q2. Author: Please provide the expansion of acronyms "CIGSe," "ITO," "PTAA," "PCBM," and "BCP," at first occurrence. 702
Q3. Author: The expanded form of the acronym "c-AFM" is given as both "atomic force microscopy in the current-sensing mode" 703
and "conductive atomic force microscope" in this paper. Please confirm that it is not at all confusing for one acronym to mean 704
two different things. 705
Q4. Author: Please check whether the edit made to the sentence "The slight modifications at the edges . . ." retains the intended 706
sense. 707
Q5. Author: Please check whether the edit made to the sentence "Successful selective laser ablation . . ." retains the intended 708
sense. 709
Q6. Author: Please check whether Ref. [17] is okay as edited. 710
Q7. Author: Please provide the institution's name where Bernd Rech received the Ph.D. degree. 711
Q8. Author: Please provide the institution's name and the year in which Bert Stegemann received the Ph.D. degree. 712

Evidence of PbI$_2$-Containing Debris Upon P2 Nanosecond Laser Patterning of Perovskite Solar Cells

Christof Schultz [ID], Felix Schneider, Antje Neubauer, Andreas Bartelt, Marko Jošt, Bernd Rech,
Rutger Schlatmann [ID], Steve Albrecht, and Bert Stegemann

Abstract—**Laser-based patterning for monolithic serial interconnection of metal halide perovskite (MHP) solar cells is a key process for industrial manufacturing of large-scale MHP solar panels. It requires reliable patterning process parameters to achieve low interconnection losses and, thus, high efficiencies. Here, P2 laser patterning of the perovskite layer was obtained by laser ablation using conventional nanosecond laser pulses at systematically varied laser fluences. The correlation of the laser impact to the morphology, composition, and electrical functionality was analyzed in detail by several surface-analytical techniques. The occurrence of laser-induced periodic surface structures and microdroplets at the bottom of the trenches indicates that material removal via stress-assisted ablation is strongly influenced by thermal processes. The formation of PbI$_2$-containing residuals was evidenced, possibly causing contact resistance losses through the P2 interconnect. These results contribute to the identification of loss factors in laser-based serial interconnection of perovskite solar cells and to further process optimization for upscaling to industrial module sizes.**

Index Terms—**Ablation, debris, laser, perovskite, P2, patterning, residuals.**

I. INTRODUCTION

INORGANIC–ORGANIC metal halide perovskites (MHPs) are very promising candidates for absorbers in low-cost solar cells [1], [2]. The main reason is its outstanding physical properties such as strong optical absorption, high charge carrier mobility, and excellent diffusive transport properties [3]. Perovskites solar cells use an absorber layer of general ABX$_3$ stoichiometry with a wide compositional range of compounds, where A = methylammonium (MA), formamidinium (FA), cesium (Cs) and B = Pb^{2+}, Sn^{2+}, Ge^{2+}, Ni^{2+}; X = iodine (I), bromine (Br), chlorine (Cl) are most commonly used [4], allowing for a tunability of the bandgap by variation of the composition [4], [5]. Thus, MHP solar cells have not only been identified as promising candidates for single-junction solar cells, but also for stacked tandem devices with one or two perovskite absorber layers [1], [4], [6]. Due to extensive research, initial power conversion efficiencies (PCE) greater than 22% [7] and stabilized efficiencies above 20% were achieved at laboratory scale with solution-processed solar cells [8].

The upscaling from small laboratory scales to industry relevant sizes requires serial interconnection of solar cells to increase the output voltage and to limit the current. Over the last years, laser processing has become a key technology in thin-film photovoltaics to achieve monolithic serial interconnection, which involves alternating layer deposition and layer patterning (so-called patterning steps P1, P2, P3) [9]. Thereby, the solar cell layers are patterned by very fine lines by selective material removal alternating with layer deposition. The P1 and the P3 scribes are used to isolate the back and front contact, and thereby determine the width of the cells, while the absorber-opening scribe (P2) enables the interconnection between the back contact and front contact of the adjacent cells. The area between the outer edges of the P1 and P3 lines is electrically inactive (so-called dead area). The range of the dead area might extend up to 100 μm away from the scribe and, thus, be notably larger than visual inspection suggests [10]. However, in order to achieve a high aperture ratio, the dead area should be as small as possible. The beneficial utilization of lasers allows highly reproducible patterning, and thereby it is advantageous in comparison to conventional needle-based patterning in terms of tool wear, accuracy, and process quality [11].

For common thin-film technologies, such as thin-film Si and CIGSe, the interaction of the laser irradiation with the specific constituent layers has been extensively studied [10], [12], and laser patterning is well-established even in industrial production [13]. However, the fabrication of large-area perovskite solar modules requires additional engineering efforts to

customize these well-established process parameters and to properly interconnect adjacent cells. In general, successful P1 and P3 patterning is characterized by a sufficiently high isolation resistance across the corresponding scribe, whereas successful P2 patterning requires a clean and smooth bottom of the trench—in order to enable lowest contact resistances—without damages of the underlying front contact layer or modified edges of the surrounding absorber material.

A few groups have reported already on successful laser-based serial interconnection and perovskite minimodule fabrication. A first monolithically series interconnected minimodule based on the mesoporous perovskite cell concept was presented in 2014 by Matteocci *et al.* reaching a PCE of $\sim$5.1% at an aperture area of $\sim$10 cm^2 [14]. At this early state, the interconnection was enabled by means of lift-off, chemical etching the P2 and masking of the P3 step. In 2015, Razza *et al.* showed a 100 cm^2 mesoporous MHP minimodule with a PCE of 4.3% [15]. Thereby, P2 patterning was carried out by a combination of lift-off and laser processing, the cell area was defined by masking. In the same year, a first fully laser-patterned minimodule was presented by Moon *et al.* reaching a PCE of about 6.6% at 5 cm^2 mesoporous MHP absorber material [16]. Palma *et al.* even increased the aperture area of the mesoporous perovskite absorber layer up to 14.5 cm^2 achieving 9.3% efficiency and a rather high aperture ratio of 95%. Recently, IMEC and Solliance [17] published their latest results and achieved a PCE of 12.4% at a 16 cm^2 minimodule, presumable also with a mesoporous structured perovskite absorber. According to these very promising results, particularly the ablation of the absorber layer by means of the P2 scribe appears still challenging and is apparently the origin of a distinct performance drop due to resistive losses, when advancing from the cell to module. Moreover, the shown rather low open-circuit voltages (V_{oc}) and comparatively low fill factor (FF) underline the assumption of resistive losses between neighboring cells, most likely due to laser-related effects, including debris- and laser-induced damage of the underlying layer.

Apparently, the P2 patterning is challenging for all laser-based approaches apparently irrespective of the cell concept (meso-porous, planar) or the MHP absorber composition, though most work has been focused yet on the mesoporous concept. Thus, it is assumed that the thermal sensitivity of the inorganic–organic perovskite compound [18], [19] might impair successful P2 laser patterning. Palma *et al.* [20] recommend a rather broad P2 scribe line, similar to the approach of Moon *et al.* [16], whereas Turan *et al.* [21] prefer multipassing in order to overcome high series resistances and to enable low-contact resistances by P2 patterning.

Thus, the objective of this work is to deliberately control the thermal impact of nanosecond (ns) laser pulses for the preparation of the P2 interconnects by optimization of the incident laser fluence, with the focus on the planar perovskite cell concept. Moreover, we aim to elucidate the results of the laser–matter interaction and to understand their correlation to the morphological, chemical, electrical, and structural properties of the laser-patterned area. Particular emphasis is put on the characterization of the bottom of the trench, since even for scribe lines, which are visually free of debris, residuals created by the laser impact are assumed to remain impeding a low contact
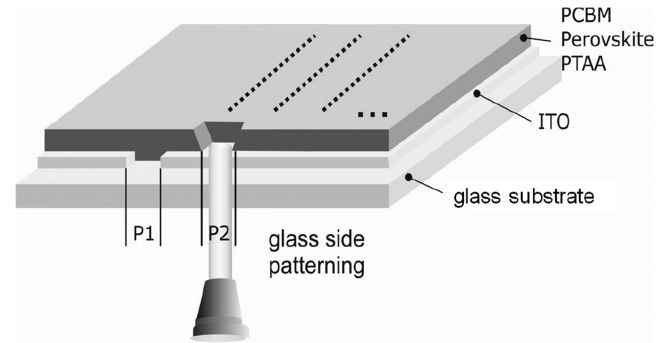

Fig. 1. Schematic illustration of the experimental approach. Multiple lines were patterned into the perovskite layer by using ns laser pulses at systematically varied energy densities.

resistance. Thus, the determination and localization of these residuals are considered to be essential to optimize the laser patterning processes. In accordance with the well-established patterning process for amorphous silicon, the P2 laser patterning for the perovskite-based cells was carried out from the glass side by means of a cost-effective nanosecond (ns) laser. The avoidance of plasma shielding [22] and the advantage of mechanically stress-assisted disintegration [23] enable selective ablation of the layer and make the glass side patterning regime putatively preferable.

Fig. 1 shows schematically the utilized sample layout, the P2 scribes were patterned line by line with systematically varied fluences.

For spatial analysis of the local conductivity, atomic force microscopy in the current-sensing mode (c-AFM) was chosen since it is a very efficient and versatile technique, which can be used to obtain locally resolved information about the morphology and the vertical conductivity between the AFM tip and to the substrate. The residuals were investigated by means of scanning electron microscope (SEM) images evaluating the morphology of the P2 bottom, whereas energy dispersive x-ray analysis (EDX) gives information about modifications of the local material composition. Moreover, the alteration of the composition of the absorber material within the trench is allocated to a new (stable) compound, and its relative composition as a function of the applied fluence is shown. Photoluminescence (PL) imaging was utilized for the locally resolved analysis of the optoelectronic properties, such as recombination processes and optical bandgaps, particularly at the bottom of the trenches and the surrounding material.

II. EXPERIMENTAL DETAILS

A. Sample Preparation

The perovskite solar cell deposition process was carried out by spin coating, resulting in a high reproducibility of the PCE on the 18% efficiency level, based on optimized deposition protocols from previous reports [24], [25]. For our experiments here, we fabricated two different sample designs in so-called "inverted" planar architecture (i.e., p–i–n geometry). First, methylammonium lead iodide (MAPbI$_3$) perovskite solar cells, using lead acetate and methylammonium iodide as precursors [25].

Parameter	
Wavelength (λ)	532 nm
Pulse duration (τ_p)	~ 30 ns
Diameter ($2\omega_0$)	28 µm ± 5 %
Pulse energy (E_p)	1.6 – 12.3 µJ
Fluence (F)	0.5 – 4.2 J/cm²
Overlap (OL)	~ 65%

The solar cell layer configuration was 1.1 mm glass, 140 nm ITO, 5 nm PTAA (hole selective contact), 270 nm perovskite, 50 nm PCBM, and 5 nm BCP (electron selective contact) [26]. Due to the continuous optimization of the perovskite preparation, we also investigated a "triple cation" perovskite sample consisting of a mixture of lead compounds (PbI$_2$/PbBr$_2$) and methylammonium bromide (MABr), formamidinium iodide (FAI), and cesium iodide (CsI) salts with a composition of Cs$_{0.05}$ (MA$_{0.17}$FA$_{0.83}$) $(100x)$ Pb $(I_{0.83}Br_{0.17})_3$, which enables higher efficiency and stability against photochemical degradation [27]. The layer configuration of these samples is 1.1 mm glass, 120 nm ITO, 5 nm PTAA, ~700 nm perovskite, 23 nm C$_{60}$ plus 8 nm BCP, with C$_{60}$ and BCP thermally evaporated. For both sample designs, 100 nm Ag is deposited onto the stack via thermal evaporation as a counter electrode. The whole preparation was carried out under nitrogen atmosphere at atmospheric pressure to avoid absorber degradation [28].

B. Laser Patterning

For laser patterning of the solar cell layers, a patterning tool (Rofin Baasel Lasertech) equipped with a high-speed motion system was used. This system consists of high-precision linear motor drives for the *x–y* translation. The stages can be moved with velocities of up to 1.2 m/s. The patterning was carried out with an ns laser source emitting pulses with durations of about $\tau_p \approx 30$ ns at a wavelength of 532 nm. This wavelength is preferable for glass side patterning, due to the high transparency of the glass and the high absorption of this wavelength within the perovskite layer supporting the mechanically stress-assisted ablation [22]. Maximum pulse energy of 45 µJ is achieved at a repetition rate of 20 kHz, which can be varied up to 400 kHz, the spatial intensity distribution is Gaussian. The patterning was done line-by-line with systematically varied laser pulse energies, covering the range of incomplete ablation of the absorber layer up to the onset of front contact damaging. The applied laser fluence ranges from 0.5 to 4.2 J/cm^2 related to a laser beam diameter of $2\omega_0 \approx (28 \pm 5) \mu$m. The pulse-to-pulse overlap (OL) was around 65% with respect to $2\omega_0$ at a pulse repetition rate of 20 kHz and was kept constant for all patterned lines. This pulse-to-pulse OL was chosen on the one hand to create a large interconnection area with minimal waists between adjacent laser shots and on the other hand to avoid excessive thermal input at the surrounding material and underlying ITO. An overview of the applied patterning parameters is given in Table I.

C. Characterization Techniques

The morphology and local conductivity of the P2 scribe were measured by a conductive atomic force microscope (c-AFM, NT-MDT NTEGRA) in the current sensing mode using a highly nitrogen-doped diamond tip. The surface was scanned at areas up to 50 μm × 50 μm under a bias voltage of 2 V, and the topography as well as the current signal was recorded simultaneously. For visual inspections of the laser patterns and modifications of the sample surface, a laser confocal microscope (OM, Keyence, VK-X250K) and an SEM (Hitachi S4100) were used. The latter one also enables the local detection of the elemental composition of the sample by means of EDX spectroscopy; the acceleration voltage was set to 5 kV. For detection of the spectrally resolved PL, a commercially available laser scanning microscope (Becker & Hickl, Simple-Tau) was used. The samples were excited by a ps laser at a wavelength of 2.63 eV (473 nm), which is well above the bandgap energy of the perovskite ~1.6 eV (~775 nm). Spectrally selective detection of the PL signal of the samples was done by specific filters.

III. RESULTS AND DISCUSSION

To open the absorber layer for monolithic interconnection, the P2 laser patterning was carried out through the glass substrate, as schematically shown in Fig. 1, with ns pulses at 532 nm. Thus, one can make use of the high difference between the absorptions coefficients of the front contact layer and the perovskite layer at 532 nm, which facilitates mechanical stress assisted ablation. For the P2 scribe, it is important to create a sufficiently large contact area for the interconnection of adjacent cells to enable low contact resistances. Therefore, a relatively high pulse-to-pulse OL is necessary. Furthermore, the bottom of the trench must be free of residuals, which might impede low contact resistances down to the front contact layer. To identify the optimal process window, the applied laser power was systematically varied, covering the range from incomplete ablation of the absorber layer $(0.5 \, \text{J/cm}^2)$ to the onset of ablation of the underlying ITO front contact layer $(4.2 \, \text{J/cm}^2)$. Thus, multiple lines were patterned in the perovskite layer, which was subsequently characterized by c-AFM, which is a powerful technique for probing local conductivity variations in heterogeneous samples with high spatial resolution [29]. Information on the local electronic properties is obtained by applying a bias voltage between the tip and the sample and sensing the resulting current. To identify optimal scribing conditions, the morphology of the sample surface as well as the spatially resolved, vertical conductivity was analyzed. A high current corresponds to a high conductivity.

The values of the average conductivity within the trenches for all applied laser fluences are summarized in the graph in Fig. 2. The results show that the conductivity increases within increasing fluence (up to a fluence of ~1.5 J/cm^2) due to the ablation of the perovskite and the exposure of the ITO. Beyond 1.5 J/cm^2, the perovskite layer is completely ablated and an alteration of the ITO sets in, resulting in a decrease of the local conductivity.

Fig. 3(a) shows the morphology of the P2 scribe and its vicinity patterned with a laser fluence of 1.53 J/cm^2. The image shows a homogeneous trench with a nearly constant width of about
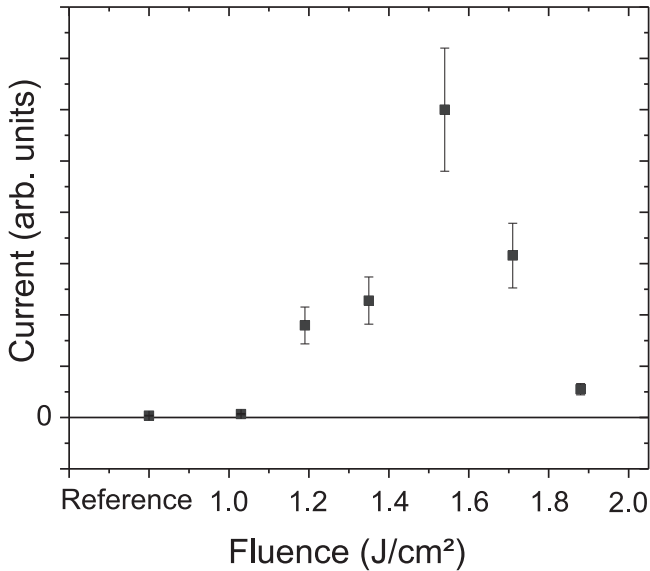
Fig. 2. Current between sample surface and c-AFM tip as a function of the applied laser fluence. The data points correspond to the average value within the laser-treated area.

35 μm. The bottom appears clean and smooth as it is preferable for low-ohmic contact resistances. The slight modifications at the edges of the trench may result from the lateral heat flux during the patterning process and give a hint that lateral thermal effects might superimpose the mechanically stress-assisted ablation as it is known from glass side patterning of, e.g., amorphous silicon thin films [23]. Following this observation, the absorption of the laser energy not only results in mechanical stress and subsequent ablation but also in heating of the perovskite layer leading to decomposition and melting of the perovskite film.

The corresponding current image is obtained by applying a bias voltage between the tip and the ITO contact and sensing the resulting current. As shown in Fig. 3(b), it visualizes a clear difference in the local conductivity between the center of the bottom trench and the untreated area, due to the removal of the perovskite and the exposure of the ITO layer. Moreover, at the bottom of the trench, alternating regions with higher and lower conductivity are found, indicating the formation of a surface texture, which is not visible in the topography image [see Fig. 3(a)]. The cross-sectional SEM image in Fig. 4 shows the edge and the center of a trench patterned at an even higher fluence of 4.2 J/cm^2.

Here, the surface texture is clearly visible and can be identified as laser-induced periodic surface structures (LIPSS) [30], which are known to be formed by laser irradiation over a wide range of materials and laser process parameters particularly at high pulse-to-pulse OL [22], as was used for P2 patterning. Such structures are understood to originate from the interference of the incident laser light with the reflected or scattered light [31]. The LIPSS periodicity is approximately 580 nm and, thus, in the same order of the incident laser wavelength. Since these periodic structures also appear both in the SEM and the c-AFM image [cf., Fig. 3(b)], it is concluded that there is an incomplete material removal of the perovskite layer and an
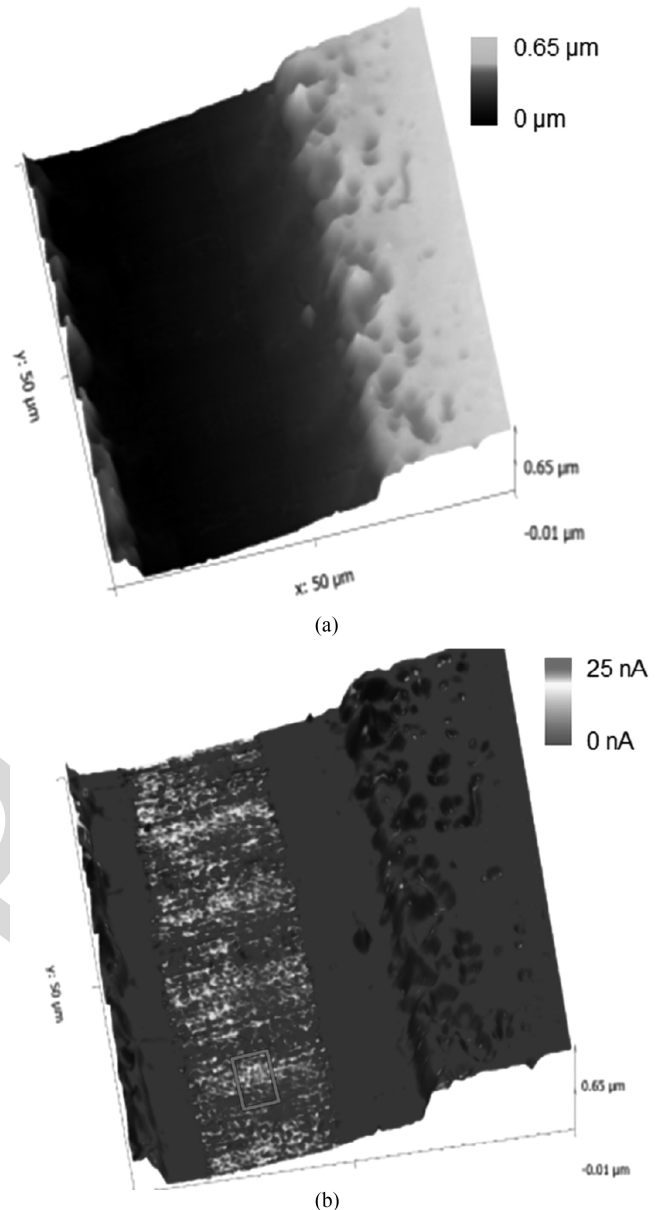

Fig. 3. (a) AFM topography. (b) Corresponding conductivity three-dimensional plots of a P2 laser-patterned trench, patterned at a fluence of 1.53 J/cm^2.

elemental redistribution leading to the periodic formation of phases with different conductivities, what can be understood by the low melting points of lead and iodine (600 and 386 K) [32] and the low sublimation temperature of the organic compound [33]. We estimated for the ns laser pulses, even for fluences below 1.5 J/cm^2, that local temperatures might reach several hundreds of Kelvin above room temperature, which affects mainly the organic part of the perovskite compound and leads to a transformation into PbI$_2$.

This interpretation is further supported by the identification of droplets on the top of the front contact layer, as revealed in the SEM image in Fig. 4 for the sample patterned at high laser fluence. From these findings, it is concluded that for ns-laser-based P2 patterning, the material removal via stress-assisted ablation is strongly influenced by thermal processes.
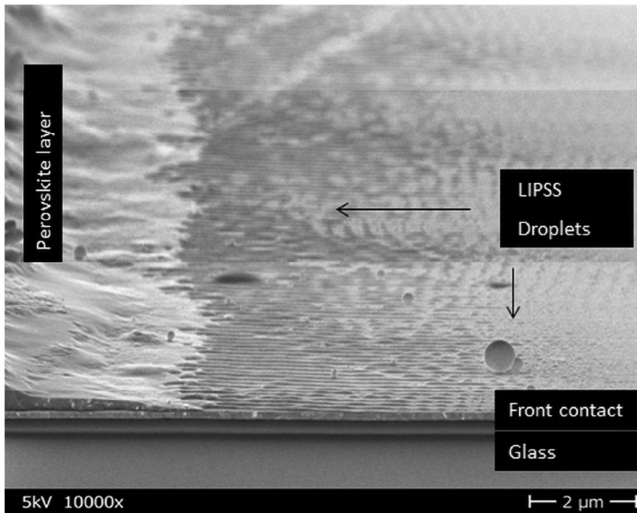
Fig. 4. SEM cross-section image of the edge and bottom of the laser scribed line, patterned at 4.2 J/cm^2. Image width: 12 μm, tilt: 10°, and acceleration voltage: 5 kV.
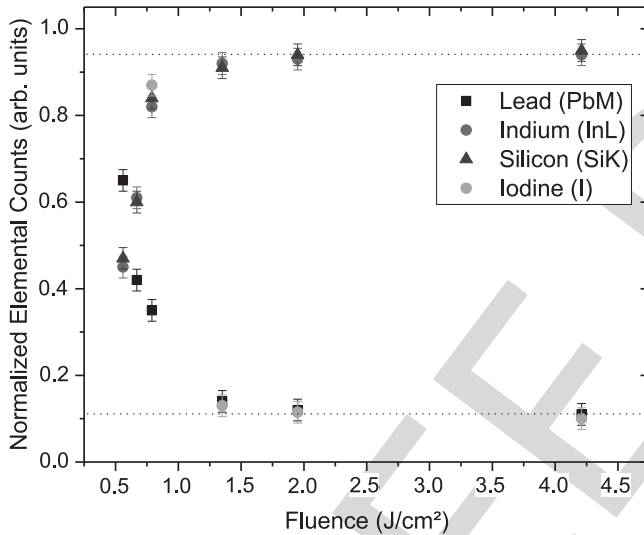

Fig. 5. Elemental composition within the P2 laser scribes as a function of the applied laser fluence. Shown are the elements I, In, Pb, and Si.

Fig. 6. Photoluminescence images of a P2 trench, patterned at 1.9 J/cm^2, revealing the emission originating. (a) Perovskite. (b) PbI$_2$. Spectral selectivity was achieved by specific filters. (a) 665 nm long pass. (b) 510/40 nm bandpass. Characteristic profiles across the P2 laser trenches correspond to the white lines and are given below the images.

To determine the elemental composition of the residuals at the bottom of the trench, all scribed lines were investigated by EDX.

Fig. 5 shows the corresponding elemental composition of the scribed lines as a function of the applied laser fluence as obtained from the relative peak intensities of the relevant elements.

As elemental references for the material composition within the scribed lines, the elements Pb, I, In, and Si were selected. Therefore, Pb and I represent the absorber materials, In the front contact, and Si the glass substrate. The results in Fig. 5 show that with increasing laser fluence the MHP layer is ablated. While the Pb and I concentration decreases with higher fluence, the In and the Si concentrations increase in the same way. However, even at high fluence, a Pb signal (about 10% of the total amount) is detected, indicating Pb-containing residuals at the bottom of the scribe.

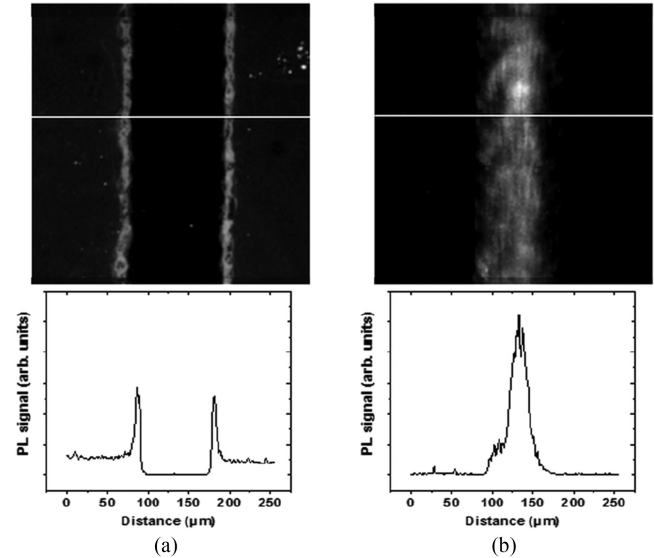With respect to the periodic structures shown in Figs. 3 and 4, it will be now clarified if the higher conductivity is due to remaining well-conducting lead-rich phases or to regions where the front contact is exposed and the remaining residuals impede a high conductivity (low contact resistance). To address this issue, spectrally resolved PL imaging was performed. The corresponding images of a sample prepared at a fluence (1.9 J/cm^2) close to the one resulting in the conductivity maximum (1.5 J/cm^2) are shown in Fig. 6.

The PL distribution of a P2 scribing line and its vicinity after filtering with a long-pass filter that transmits wavelengths above 665 nm is shown in Fig. 6(a). Thus, the emission of the main transition of the perovskite layer at 780 nm (1.59 eV) is detected. The line scan below corresponds to the white line in the PL image and shows that at the bottom of the trench the PL signal of the perovskite vanishes, indicating the absence of perovskite. A further distinct feature is the raised PL intensity at the edges of the scribed line, which can be attributed to the removed electron extraction layer (C$_{60}$/PCBM) close to the scribe allowing for an increased perovskite PL intensity [24]. Further analysis of the edges by means of confocal optical microscopy shows only very little ridges; thus, focus-related effects regarding the signal detection can be excluded. However, further investigations to quantify this effect are in progress.

In contrast, the PL image in Fig. 6(b) was acquired using a bandpass filter with a nominal center wavelength of 510 nm and a bandwidth of 40 nm. This filter enables the detection of the PL signal of PbI$_2$ (main transition at 529 nm at 300 K [34]) while blocking the PL signal of the perovskite. As is seen, a distinct PL signal is found within the scribed line, apparently originating from PbI$_2$-based residuals, which are formed upon laser impact and remain in the trench after P2 laser patterning. This interpretation is in agreement with x-ray diffraction

measurements by Bayer *et al.*, who observed structural decomposition of MHP due to ns laser patterning, resulting in the formation of PbI$_2$ [35]. PbI$_2$ formation in lead-containing perovskite layers has been focused a lot of attention and its role for the performance of the device has been controversially discussed. It was proposed that a degradation of the lead-containing perovskite to PbI$_2$ might occur in air or vacuum, with excessive heat or humidity facilitating this process [36]. Some beneficial effects are ascribed to the presence of PbI$_2$, such as passivation of perovskite grain boundaries [37], [38], increasing the shunt resistance of the active layer and reducing the ion mobility [39]. However, detrimental effects on the photostability were also found to be caused by excess PbI$_2$ [40]. Moreover, ns P2 laser ablation was observed to be followed by redeposition of ablated material.

Taking all this observation into account, we conclude that thermal effects lead to the decomposition of the organic/inorganic hybrid material resulting in a formation of PbI$_2$ with a periodically structured morphology and possibly the redeposition of PbI$_2$ debris. Thus, it must be assumed that the remaining PbI$_2$ within the trench might act as a barrier for the charge carrier transport [37] due to its rather high resistivity of 10^8–10^{10} $\Omega\cdot$cm [41], [42] and its comparatively large band gap of 2.34 eV [34], thus impeding low-contact resistances. These findings can be generalized to all investigated absorber layer compositions in the "inverted" planar architecture. Process windows and results from SEM and EDX measurements are consistent. Even the slightly thicker absorber layer used for the triple cation sample has a negligible influence on the absorption behavior.

IV. SUMMARY AND CONCLUSION

P2 laser patterning through the glass substrate by ns laser pulses for monolithic series interconnection of MHP solar cells was investigated over a wide range of laser fluences. Successful selective laser ablation from the glass side is demonstrated, though at the bottom of the scribed lines periodically structured, residual composed of PbI$_2$ remains even at higher fluences. These features form periodic surface structures (LIPSS), which exhibit regions of higher and lower conductivity, and thus impede low contact resistances for the P2 interconnect. It is concluded that the comparatively poor conductivity of PbI$_2$ hinders lower contact resistances as they are essential for successful monolithic series interconnection.

The occurrence of LIPSS and in addition microdroplets at the uncovered front contact layer indicate that material removal for P2 patterning via stress-assisted ablation is strongly influenced by thermal processes. Thus, further extensive work is required to overcome these drawbacks and to adjust the process windows for industrial manufacturing. Currently, further process optimization is in progress evaluating shorter laser pulse durations to avoid thermal effects (i.e., heat accumulation) and different wavelengths for material excitation above and below the optical bandgap to further improve P2 patterning and to achieve lowest contact resistances.

REFERENCES

[1] S. Albrecht *et al.*, "Monolithic perovskite/silicon-heterojunction tandem solar cells processed at low temperature," *Energy Environ. Sci.*, vol. 9, pp. 81–88, 2016.

[2] E. L. Unger, "The PV-researcher's siren: Hybrid metal halide perovskites," *Curr. Opinion Green Sustain. Chem.*, vol. 4, pp. 72–76, 2017.

[3] J. S. Manser, J. A. Christians, and P. V. Kamat, "Intriguing optoelectronic properties of metal halide perovskites," *Chem. Rev.*, vol. 116, pp. 12956–13008, 2016.

[4] E. L. Unger *et al.*, "Roadmap and roadblocks for the band gap tunability of metal halide perovskites," *J. Mater. Chem. A*, vol. 5, pp. 11401–11409, 2017.

[5] Q. A. Akkerman *et al.*, "Tuning the optical properties of cesium lead halide perovskite nanocrystals by anion exchange reactions," *J. Amer. Chem. Soc.*, vol. 137, pp. 10276–10281, 2015.

[6] T. Todorov *et al.*, "Monolithic perovskite-CIGS tandem solar cells via in situ band gap engineering," *Adv. Energy Mater.*, vol. 5, 2015, Art. no. 1500799.

[7] N.-G. Park, "Methodologies for high efficiency perovskite solar cells," *Nano Convergence*, vol. 3, pp. 1–13, 2016.

[8] Ecole Polytechnique Fédérale de Lausanne, "Perovskite solar cells reach record long-term stability, efficiency over 20%," Science Daily, 2017.

[9] A. Compaan, I. Matulionis, and S. Nakade, "Optimization of laser scribing for thin-film PV modules," Univ. Toledo, Toledo, OH, USA, Final Tech. Prog. Rep., 1998, p. 43.

[10] C. Schultz *et al.*, "Revealing and identifying laser-induced damages in CIGSe solar cells by photoluminescence spectroscopy," *IEEE J. Photovolt.*, vol. 7, no. 5, pp. 1442–1449, Sep. 2017.

[11] L. Rakocevic *et al.*, "Interconnection optimization for highly efficient perovskite modules," *IEEE J. Photovolt.*, vol. 7, no. 1, pp. 404–408, Jan. 2017.

[12] C. Schultz *et al.*, "Laser-induced local phase transformation of CIGSe for monolithic serial interconnection: Analysis of the material properties," *Sol. Energy Mater. Sol. Cells*, vol. 157, pp. 636–643, 2016.

[13] G. Heise, A. Heiss, H. Vogt, and H. P. Huber, "Ultrafast lasers improve the efficiency of CIS thin film solar cells," *Phys. Procedia*, vol. 39, pp. 702–708, 2012.

[14] F. Matteocci *et al.*, "Solid-state solar modules based on mesoscopic organometal halide perovskite: A route towards the up-scaling process," *Phys. Chem. Chem. Phys.*, vol. 16, pp. 3918–3923, 2014.

[15] S. Razza *et al.*, "Perovskite solar cells and large area modules (100 cm^2) based on an air flow-assisted PbI$_2$ blade coating deposition process," *J. Power Sources*, vol. 277, pp. 286–291, 2015.

[16] S.-J. Moon *et al.*, "Laser-scribing patterning for the production of organometallic halide perovskite solar modules," *IEEE J. Photovolt.*, vol. 5, no. 4, pp. 1087–1092, Jul. 2015.

[17] IMEC and Solliancce, "IMEC and Solliance's perovskites PV modules achieve 12.4%," 2017. [Online]. Available: https://solliance.eu/perovskite-modules-achieve-12-4pct/

[18] E. J. Juarez-Perez, Z. Hawash, S. R. Raga, L. K. Ono, and Y. B. Qi, "Thermal degradation of CH$_3$NH$_3$PbI$_3$ perovskite into NH$_3$ and CH$_3$I gases observed by coupled thermogravimetry-mass spectrometry analysis," *Energy Environ. Sci.*, vol. 9, pp. 3406–3410, 2016.

[19] A. E. Williams *et al.*, "Perovskite processing for photovoltaics: A spectro-thermal evaluation," *J. Mater. Chem. A*, vol. 2, pp. 19338–19346, 2014.

[20] A. L. Palma *et al.*, "Laser-patterning engineering for perovskite solar modules with 95% aperture ratio," *IEEE J. Photovolt.*, vol. 7, no. 6, pp. 1674–1680, Nov. 2017.

[21] B. Turan, A. Huuskonen, I. Kühn, T. Kirchartz, and S. Haas, "Cost-effective absorber patterning of perovskite solar cells by nanosecond laser processing," *Solar RRL*, vol. 1, 2017, Art. no. 1700003.

[22] D. W. Bäuerle, *Laser Processing and Chemistry*. New York, NY, USA: Springer, 2013, p. 281.

[23] J. Bovatsek, A. Tamhankar, R. Patel, N. Bulgakova, and J. Bonse, "Thin film removal mechanisms in ns-laser processing of photovoltaic materials," *Thin Solid Films*, vol. 518, pp. 2897–2904, 2010.

[24] L. Kegelmann *et al.*, "It takes two to tango – Double-layer selective contacts in perovskite solar cells for improved device performance and reduced hysteresis," *ACS Appl. Mater. Interfaces*, vol. 9, pp. 17245–17255, 2017.

[25] M. Jošt *et al.*, "Efficient light management by textured nanoimprinted layers for perovskite solar cells," *ACS Photon.*, vol. 4, pp. 1232–1239, 2017.

[26] M. Stolterfoht *et al.*, "Approaching the fill factor Shockley-Queisser limit in stable, dopant-free triple cation perovskite solar cells," *Energy Environ. Sci.*, vol. 10, pp. 1530–1539, 2017.

[27] M. Saliba *et al.*, "Cesium-containing triple cation perovskite solar cells: Improved stability, reproducibility and high efficiency," *Energy Environ. Sci. Adv.*, vol. 9, pp. 1989–1997, 2016.

[28] Z. Song *et al.*, "Perovskite solar cell stability in humid air: Partially reversible phase transitions in the PbI_2-CH_3NH_3I-H_2O system," *Adv. Energy Mater.*, vol. 6, 2016, Art. no. 1600846.

[29] B. Stegemann, J. Čermák, B. Rezek, J. Kočka, and M. Schmidt, "Silicon nanodot layers for photovoltaic application: Size/Density control and electrical properties," *Zeitschrift Phys. Chem.*, vol. 228, pp. 543–556, 2014.

[30] J. Bonse, S. Höhm, S. Kirner, A. Rosenfeld, and J. Krüger, "Laser-induced periodic surface structures (LIPSS) - A scientific evergreen," *IEEE J. Sel. Top. Quantum Electron.*, vol. 23, no. 3, May/Jun. 2017, Art. no. 9000615.

[31] K. Sugioka and Y. Cheng, "Ultrafast lasers - Reliable tools for advanced materials processing," *Light Sci. Appl.*, vol. 3, 2014, Art. no. e149.

[32] W. M. Haynes, *CRC Handbook of Chemistry and Physics*. Boca Raton, FL, USA: CRC Press, 2014.

[33] A. Dualeh, P. Gao, S. I. Seok, M. K. Nazeeruddin, and M. Grätzel, "Thermal behavior of methylammonium lead-trihalide perovskite photovoltaic light harvesters," *Chem. Mater.*, vol. 26, pp. 6160–6164, 2014.

[34] R. Ahuja *et al.*, "Electronic and optical properties of lead iodide," *J. Appl. Phys.*, vol. 92, pp. 7219–7224, 2002.

[35] L. Bayer *et al.*, "Morphology and topography of perovskite solar cell films ablated and scribed with short and ultrashort laser pulses," *Appl. Surf. Sci.*, vol. 416, pp. 112–117, 2017.

[36] Q. Sun *et al.*, "Role of microstructure in oxygen induced photodegradation of methylammonium lead triiodide perovskite films," *Adv. Energy Mater.*, vol. 7, 2017, Art. no. 1700977.

[37] T. J. Jacobsson *et al.*, "Unreacted PbI_2 as a double-edged sword for enhancing the performance of perovskite solar cells," *J. Amer. Chem. Soc.*, vol. 138, pp. 10331–10343, 2016.

[38] L. Wang, C. McCleese, A. Kovalsky, Y. Zhao, and C. Burda, "Femtosecond time-resolved transient absorption spectroscopy of $CH_3NH_3PbI_3$ perovskite films: Evidence for passivation effect of PbI_2," *J. Amer. Chem. Soc.*, vol. 136, pp. 12205–12208, 2014.

[39] T. Du *et al.*, "Formation, location and beneficial role of PbI_2 in lead halide perovskite solar cells," *Sustain. Energy Fuels*, vol. 1, pp. 119–126, 2017.

[40] F. Liu *et al.*, "Is excess PbI_2 beneficial for perovskite solar cell performance?" *Adv. Energy Mater.*, vol. 6, 2016, Art. no. 1502206.

[41] H. Henisch and C. Srinivasagopalan, "Properties of semiconducting lead iodide," *Solid State Commun.*, vol. 4, pp. 415–418, 1966.

[42] C. De Blasi *et al.*, "Trapping levels in PbI_2," *Solid State Commun.*, vol. 25, pp. 149–153, 1978.

Felix Schneider received the bachelor's degree in renewable energies from the University of Applied Sciences (HTW) Berlin, Germany, in 2015, and the master's degree in renewable energies in 2017 from the HTW Laser Research Group, Competence Center Thin-Film- and Nanotechnology for Photovoltaics Berlin, Berlin, Germany, where he focused on the serial interconnection of perovskite solar cells via laser patterning.

During his thesis, he worked with the PI Photovoltaik Institut Berlin, Berlin, Germany, on solar module testing and evaluation. Since 2018, he has been working with the TÜV Rheinland Industrie Service, Berlin, Germany.

Antje Neubauer studied chemistry at Humboldt University, Berlin, Germany. She received the Ph.D. degree in physics from Technical University, Cottbus, Germany, in 2010.

She worked in ultrafast spectroscopy of dye-sensitized solar cells with Helmholtz Centre Berlin, Berlin, Germany. Subsequent postdoctoral positions at Helmholtz Centre Berlin and University of Rostock focused on time-resolved spectroscopy of solar energy materials. Since 2015, she has been an Application Scientist for time-correlated single photon counting with Becker & Hickl GmbH, Berlin, Germany.

Andreas Bartelt received the Ph.D. degree from the Free University of Berlin, Berlin, Germany, where he focused on laser-driven chemistry induced by tailored femtosecond laser pulses.

He works in the field of laser chemistry and material sciences. Time-resolved spectroscopy using lasers and synchrotron x-rays was at the core of his Postdoctoral research at Princeton University, Lawrence Berkeley National Laboratories, and Helmholtz Center Berlin, investigating novel thin-film photovoltaic materials. He has been a Full Professor with the University of Applied Sciences, Berlin, Germany, since 2016. His main research interests include femtosecond spectroscopy and material processing of organic–inorganic hybrid and perovskite solar cells.

Christof Schultz received the diploma and master's degrees in renewable energies from the University of Applied Sciences, Berlin, Germany, in 2008 and 2014, respectively.

In 2010, he joined the HTW Laser Research Group, Competence Center Thin-Film- and Nanotechnology for Photovoltaics Berlin, Berlin, Germany, as a Specialist for laser applications. His current research interests include laser processing, laser spectroscopy, and characterization of CIGSe solar cells; for his Ph.D. studies, he focused on laser patterning of inorganic–organic perovskite solar cells as well as laser-induced damages in order to optimize the laser patterning.

Marko Jošt received the Ph.D. degree from the University of Ljubljana, Ljubljana, Slovenia, and Technical University Berlin, Berlin, Germany, where he investigated light management in solar cells.

He is currently a Postdoctoral Researcher with the Young Investigator Group Perovskite Tandem Solar Cells, Helmholtz-Zentrum Berlin, Berlin, Germany. His current research interest focuses on improving the efficiency of monolithic perovskite/silicon tandem solar cells, with an emphasis on optical optimization and interface engineering.

Bernd Rech studied physics at Heidelberg University, Heidelberg, Germany, and RWTH Aachen, Aachen, Germany. He received the Ph.D. degree in physics in 1997.

From 1999 to 2006, he was the Leader of a group specialized in solar cell technology with the Institute of Photovoltaics, Forschungszentrum Jülich. He was appointed as a Professor with the Faculty of Electrical Engineering and Computer Science, Technische Universität Berlin, in 2007. Since 2008, he has been the Spokesperson of the research program renewable energies of the Helmholtz Association. From 2006 to 2017, he was the Head of the Institute of Silicon Photovoltaics, Helmholtz-Zentrum Berlin (HZB), Berlin, Germany, and the Spokesperson of the division renewable energies from 2011 to 2017. He and his team focused on the development of highly efficient and affordable thin-film silicon solar cells and new material combinations for producing tandem solar cells. Since May 2017, he has been the Acting Scientific Director of the HZB.

Dr. Rech was elected member of Acatech (National Academy of Science and Engineering) in 2017.

Rutger Schlatmann received the Ph.D. degree in physics, working on X-ray multilayer mirrors, from the FOM Institute Amolf, Amsterdam, The Netherlands, in 1995.

From 1996 to 1999, he worked on high strength polymer fibers as a Research Scientist for Akzo Nobel. From 1999 to 2008, he was the R&D Manager with Helianthos BV, a company developing flexible thin-film Si solar modules. Since 2008, he has been the Director of the Center for Technology Transfer in Thin-Film- and Nanotechnology for Photovoltaics, Helmholtz-Zentrum Berlin, Berlin, Germany. Since 2012, he has held a Full Professorship (W3) with the University of Applied Sciences Berlin, Berlin, Germany. His research interests focus on all aspects of Si heterojunction and CIGS-based solar cells, including multijunction cells, new concepts for light capture and conversion (e.g., solar fuels, solar-driven hydrogen generation), alternatives to standard absorber layer formation, and on and offline analytics. His main focus is on research topics that are ready to move from proof of principle to proof of concept.

Dr. Schlatmann is a Member of the European Technology and Innovation Platform PV Steering Committee as well as the Vice President of the Berlin Brandenburg Energy Network, and a Member of various national and international conference and scientific evaluation committees.

Steve Albrecht received the Ph.D. degree in physics from the University of Potsdam, Potsdam, Germany.

He has been leading a young investigator group for perovskite-based multijunction photovoltaics at Helmholtz Center Berlin, Berlin, Germany, since 2016. In 2014, he joined Helmholtz Center Berlin, as a Postdoc until his young investigator group was founded. In 2017, he managed the build-up of the HySPRINT Innovation Lab for perovskite solar cells at Helmholtz Center Berlin, which is under operation now. Recently, his group developed a two-terminal, monolithic perovskite/silicon tandem solar cell with a certified efficiency of 25%.

Dr. Albrecht was a recipient of the Carl-Ramsauer-Prize and the Young Researcher Prize of the Berlin Physical Society and the Leibniz-Kolleg Potsdam, respectively, for his Ph.D. work on organic solar cells.

Bert Stegemann studied physics and optical sciences at the Humboldt University Berlin, Berlin, Germany, and the University of Arizona, Tuscon, AZ, USA. He received the Ph.D. degree in physical chemistry.

After completing his Ph.D. degree, he worked on several research projects in the fields of laser applications, material sciences, and photovoltaics. Since 2009, he has held a Full Professorship for photovoltaics with the University of Applied Sciences Berlin (HTW), Berlin, Germany, and is the Head of the HTW Laser Technology Lab, Competence Center Thin-Film- and Nanotechnology for Photovoltaics Berlin. His current research interests include laser processing, laser spectroscopy, and characterization of CIGSe, perovskite, and Si heterojunction solar cells as well as wet-chemical processing and interface passivation.

QUERIES 700

Q1. Author: Please confirm or add details for any funding or financial support for the research of this article. 701

Q2. Author: Please provide the expansion of acronyms "CIGSe," "ITO," "PTAA," "PCBM," and "BCP," at first occurrence. 702

Q3. Author: The expanded form of the acronym "c-AFM" is given as both "atomic force microscopy in the current-sensing mode" 703
and "conductive atomic force microscope" in this paper. Please confirm that it is not at all confusing for one acronym to mean 704
two different things. 705

Q4. Author: Please check whether the edit made to the sentence "The slight modifications at the edges..." retains the intended 706
sense. 707

Q5. Author: Please check whether the edit made to the sentence "Successful selective laser ablation..." retains the intended 708
sense. 709

Q6. Author: Please check whether Ref. [17] is okay as edited. 710

Q7. Author: Please provide the institution's name where Bernd Rech received the Ph.D. degree. 711

Q8. Author: Please provide the institution's name and the year in which Bert Stegemann received the Ph.D. degree. 712